AIAA JOURNAL
Vol. 44, No. 7, July 2006

Turbulence Models for Flows with Free Surfaces and Interfaces

Ebrahim Shirani,* Ali Jafari,† and Nasser Ashgriz‡
University of Toronto, Toronto, Ontario M5S 3G8, Canada

The Reynolds-averaged equations of motion for turbulent interfacial flows are developed. A new model for the correlation of the mean pressure with the fluctuations of the interface location is introduced. A parameter referred to as turbulent surface tension coefficient is introduced that models the effect of turbulence on increasing the surface tension force. In addition, a model for the correlation of the mean fluctuations of the volume fraction with velocity is presented. A volume-of-fluid-based model is used to simulate the dynamics of the interface between the two immiscible fluids. The new turbulence models are used to simulate a two-dimensional Kelvin–Helmholtz instability at high-Reynolds-number flows. In addition, the turbulence models are used to simulate spreading of a plane turbulent water jet in air.

Introduction

A LARGE number of flows in nature and industry involve free surfaces or material interfaces. Their applications range from environmental sciences, geophysics, and fundamental physics to numerous engineering problems. The shape of the interface (as a sharp discontinuity) plays an important role in dynamics of the problem. The accurate prediction of position, curvature, and topology of the interface is essential in simulating the problem. Numerous methods have been developed to capture the interface motion. Among these are the front tracking and volume tracking methods, which are capable of capturing large interface deformations. Almost all of these methods are designed for laminar flows, and no consideration is given to the turbulence effects. Therefore, using these methods without modifications to simulate turbulent free-surface flows cannot be a realistic and accurate treatment of the problem.

Turbulence near the interfaces separating the immiscible fluids is a very complex phenomenon involving moving boundaries, vortex interactions with the interface, rapid deformations of the interface, ligament formation, and breakup and merging of the interface. Many of these effects remain unexplained.

The effect of turbulence on the interface can be quite significant. For example, the surface normal component of the turbulent kinetic energy may be redistributed into surface parallel component. This behavior, the anisotropy of turbulence near the interface, is due to the surface tension and the gravity forces depending on the flow Weber and Froude numbers, respectively. In addition, surface deformation and vortices near the free surface can generate vorticities normal to the free surface.

Turbulence modeling of flows with interfaces is in its early stages. Some of the primary works in this area are described next. Hong and Walker[1] developed a set of Reynolds-averaged equations for free-surface flows. Their objective was to study a turbulent jet near a free surface. Using an order of magnitude analysis, they showed that, for low Froude numbers, the Reynolds stress anisotropy was mainly responsible for the outward acceleration of the surface current. For the high Froude numbers, the Reynolds stress anisotropy was smaller and the free-surface fluctuations made a significant contribution to the surface currents. Banerjee[2] derived the conservation equations for turbulent multiphase flows based on various forms of averaging. He discussed the modeling of interfacial transport processes and turbulence modifications in one phase due to the presence of the other phases. He argued that the turbulence structure near the gas–liquid interfaces depends primarily on the shear rate. Lopez de Bertodano et al.[3] and Lahey and Drew[4] employed the k–ε model for two-fluid problems. They considered the two-way coupling effects of the fluids because the turbulence in the liquid phase has a strong influence on the void fraction distribution and bubble flattening, whereas fragmentation and wobble will have feedback effects on the production of turbulent kinetic energy. Walker and Chen[5] evaluated three algebraic stress models for predicting turbulent stresses near the free surface. Lin and Liu[6] used the k–ε model along with a nonlinear Reynolds stress model to simulate breaking waves in the surf zone.

None of the previous works on the turbulence modeling of interfacial flows include the effects of pressure fluctuations on the interface itself. High-frequency turbulent pressure fluctuations near the interface may generate very large local interface curvatures, resulting in large local surface forces at the interface. In the present study, the effect of pressure fluctuations and its correlation with the interface fluctuations is considered.

There are limited studies relevant to modeling turbulent interfacial flows using Reynolds-averaged Navier–Stokes (RANS) and/or large-eddy simulation (LES) in the Eulerian formulation. A number of researchers[7,8] have pointed out that as a result of averaging process (or filtering in the case of LES), some new terms appear. The subgrid-scale surface tension term is mentioned; however, no model has been presented for it. In another study, Alajbegovic[9] has applied LES methodology to multiphase flows and has proposed relations for large-scale simulation of these flows. He has derived a general closure for the subgrid surface tension force. However, he has not provided the details of this closure term because the relationship between the closure coefficient, the flow turbulence, and the free-surface motion characteristics was not provided.

In this paper, the sheared interface between two immiscible fluids at high Reynolds numbers and the spreading of plane water jet in air are simulated. This study is the first step to simulate more complex turbulent interfacial flows. Our main objective is to introduce new ideas and models of turbulence necessary to simulate interfacial flows. A new model for correlation of the mean pressure with fluctuations of the interface location is developed in this work. In addition, the correlation of the volume fraction fluctuations with velocity is modeled, and the model is used in the volume fraction equation. The new models are applied in RANS formalism (rather than LES considered by other researchers). Because RANS, is used, many flow characteristics may not be captured directly, and the level

Presented as Paper 2004-1283 at the AIAA 42nd Aerospace Sciences Meeting, Reno, NV, 5–8 January 2004; received 15 March 2005; revision received 1 February 2006; accepted for publication 9 February 2006.

*Visiting Scientist, Department of Mechanical and Industrial Engineering; currently Professor, Department of Mechanical Engineering, Isfahan University of Technology, Isfahan 84156, Iran.

†Graduate Student, Department of Mechanical and Industrial Engineering.

‡Professor, Department of Mechanical and Industrial Engineering; ashgriz@mie.utoronto.ca.

of modeling is much higher than that for LES. Thus, these terms cannot be neglected in RANS. Note that the models presented here can be applied (with minor changes) to LES formalism as well.

We have used our proposed models to simulate the primary breakup of immiscible fluid interfaces. Some model constants are obtained by comparing the simulation results of a plane turbulent water jet injected into still air with the experimental results by Sallam et al.[10]

The governing equations for two-dimensional unsteady, incompressible flows are used in the form of the Reynolds-averaged equations. To close the time-averaged governing equations, two different turbulence models along with the new models for the fluctuation of the pressure interface location and the volume fraction–velocity correlations are used. It is assumed that the fluids are immiscible without phase change and the volume-of-fluid (VOF) method is used for capturing the interface motion.

Governing Equations

Two-dimensional incompressible time-dependent Navier–Stokes equations for a two-fluid problem including the liquid interfaces are used. It is assumed that the velocity field is continuous across the interface, but there is a pressure jump at the interface due to the surface tension. Following the VOF method,[11] the advective equation for volume fraction F is used to calculate the volume fraction and the shape of the interface.

Assuming that the timescale of the turbulent flows is small compared to the timescale of the mean flow structures at the interface, the time average of the governing equations are as follow:

$$\frac{\partial \bar{u}_i}{\partial x_i} = 0 \tag{1}$$

$$\frac{\partial \bar{F}}{\partial t} + \frac{\partial \bar{F}\bar{u}_i}{\partial x_i} + \overline{\frac{\partial F' u_i'}{\partial x_i}} = 0 \tag{2}$$

$$\frac{\partial \bar{u}_i}{\partial t} + \frac{\partial \bar{u}_i \bar{u}_j}{\partial x_j} + \frac{\partial \overline{u_i' u_j'}}{\partial x_j} = -\frac{1}{\bar{\rho}}\frac{\partial \bar{p}}{\partial x_i} + \frac{\mu}{\bar{\rho}}\left(\frac{\partial^2 \bar{u}_i}{\partial x_j \partial x_j}\right) + \frac{1}{\bar{\rho}}\overline{B_i^{\mathrm{st}}} \tag{3}$$

where ρ is density, u_i are the velocity components, t and x_i are time and space coordinates, p is pressure, B^{st} is the volumetric surface tension force, the overbar denotes the time average, and prime denotes the fluctuating quantities. In general, B^{st} can be written as $\sigma\kappa\delta_s \boldsymbol{n}$ where, σ is the surface tension coefficient, κ is the interface curvature, δ_s is Dirac delta function, and $\boldsymbol{n}$ is the unit vector normal to the interface.

The time averages of density and viscosity are

$$\bar{\rho} = \rho_2 + \bar{F}(\rho_1 - \rho_2), \qquad \bar{\mu} = \mu_2 + \bar{F}(\mu_1 - \mu_2) \tag{4}$$

respectively. The subscripts 1 and 2 denote the two fluids. Because of the fluctuations of the pressure and velocity in the transition region (the region near the interface) and the motions of eddies in this region, the interface location may fluctuate. Thus, the curvature of the interface is a turbulent quantity, and it fluctuates with time and space. In fact, the fluctuation of the interface location is related to the pressure fluctuations in this region. This suggests that the pressure and the interface location fluctuations may be well correlated and may affect the flow characteristics at the interface.

The pressure in the interfacial region with the presence of surface tension needs careful consideration. In fact, due to the sharp discontinuity of the pressure at the interface, the pressure force in the interfacial cells depends on the location of the interface at the cell faces. The following derivations give the relation for pressure at the interface.

Let us derive a relation between pressure at the cell center and the interface location in the same cell for the one-dimensional case. The pressure force per unit area F_{pL} acting on the left-hand side of an interfacial cell (Fig. 1) can be written as

$$F_{pL} = p_L(\Delta y/\Delta y) = p_{1L}(l_L/\Delta y) + [(\Delta y - l_L)/\Delta y]p_{2L} \tag{5}$$

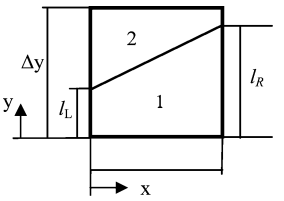

Fig. 1 Cell with interface.

or

$$F_{pL} = p_L = p_{1L}H_L + (1 - H_L)p_{2L} \tag{6}$$

where p_L is the average pressure on the left-hand side of the cell, Δy is the length of the cell in the y direction, l_L is the length of the cell side that is in contact with fluid 1, and $H_L = l_L/\Delta y$ is the ratio of the length (area) filled with fluid 1 on the left-hand side denoting the instantaneous location of the interface on the left-hand side. Equation (6) may be rearranged as

$$p_L = p_{2L} + H_L(p_{1L} - p_{2L}) \tag{7}$$

The pressure difference in the parenthesis represents the pressure jump due to the surface tension. Similar relations can be obtained for the pressure force on the right, top, and bottom sides.[12] In general,

$$p = p_2 + H(p_1 - p_2) \tag{8}$$

The time average of the pressure, Eq. (8), is

$$\bar{p} = \overline{p_2} + (\overline{p_1} - \overline{p_2})\bar{H} + \overline{(p_1' - p_2')H'} \tag{9}$$

The second term on the right-hand side of Eq. (9) corresponds to the mean values, and it is related to the molecular surface tension:

$$(\overline{p_1} - \overline{p_2})\bar{H} = \sigma\bar{\kappa}\bar{H} \tag{10}$$

where $\bar{\kappa}$ is the mean curvature of the interface. The last term in Eq. (9) introduces a mean value of fluctuating quantities that needs to be modeled. This term is responsible for the effect of pressure fluctuations at the interface, which may affect the breakup process and the generation of disturbances and waves at the interface.

Turbulence Modeling

To close the Reynolds-averaged equations, the average of fluctuating quantities appearing in Eqs. (1–3), along with Eqs. (4) and (9), must be modeled. The terms that require modeling are

$$\overline{u_i' u_j'}, \qquad \overline{F' u_i'}, \qquad \overline{(p_1' - p_2')H'} \tag{11}$$

Reynolds Stress Term

To model the first term in Eq. (11) (Reynolds stress term), two turbulence models are used: the standard two-equation k–ε model and another k–ε based model that consists of a realizable Reynolds stress algebraic equation model.[13] The latter model has significantly improved the predictive capability of k–ε based models, especially for flows involving strong shear layers. The equations for these models are

$$\frac{\partial k}{\partial t} + \bar{u}_j\frac{\partial k}{\partial x_j} = \frac{\partial}{\partial x_j}\left[\left(\upsilon + \frac{\upsilon_\tau}{\sigma_k}\right)\frac{\partial k}{\partial x_j}\right] - \overline{u_i' u_j'}\frac{\partial \bar{u}_i}{\partial x_j} - \varepsilon \tag{12}$$

$$\frac{\partial \varepsilon}{\partial t} + \bar{u}_j\frac{\partial \varepsilon}{\partial x_j} = \frac{\partial}{\partial x_j}\left[\left(\upsilon + \frac{\upsilon_\tau}{\sigma_\varepsilon}\right)\frac{\partial \varepsilon}{\partial x_j}\right] - C_{\varepsilon 1}\frac{\varepsilon}{k}\overline{u_i' u_j'}\frac{\partial \bar{u}_i}{\partial x_j} - C_{\varepsilon 2}\frac{\varepsilon^2}{k} \tag{13}$$

where k and ε are turbulent kinetic energy and its dissipation rate, respectively, and the values of coefficients are $\sigma_k = 1$, $\sigma_\varepsilon = 1.3$, $C_{\varepsilon 1} = 1.44$, and $C_{\varepsilon 2} = 1.92$. The Reynolds stresses can be written as[13]

$$\overline{u_i' u_j'} = \tfrac{2}{3}k\delta_{ij} - C_\mu(k^2/\varepsilon)2S_{ij} + 2C_2(k^3/\varepsilon^2)(-S_{ik}\Omega_{kj} + S_{kj}\Omega_{ik}) \tag{14}$$

where

$$S_{ij} = \frac{1}{2}\left(\frac{\partial u_i}{\partial x_j} + \frac{\partial u_j}{\partial x_i}\right) - \frac{1}{3}\frac{\partial u_k}{\partial x_k}\delta_{ij}, \qquad \Omega_{ij} = \frac{1}{2}\left(\frac{\partial u_i}{\partial x_j} - \frac{\partial u_j}{\partial x_i}\right) \tag{15}$$

and the kinematic eddy viscosity υ_τ is related to k and ε according to

$$\upsilon_\tau = C_\mu(k^2/\varepsilon) \tag{16}$$

where $C_\mu = 0.09$ and $C_2 = 0$ for the standard k–ε model. For the algebraic model, these coefficients are

$$C_\mu = \frac{1}{6.5 + A(Uk/\varepsilon)}$$

$$C_2 = \frac{\sqrt{1 - 9S_{ij}S_{ij}C_\mu^2(k/\varepsilon)^2}}{1 + 6\left(\sqrt{S_{ij}S_{ij}}k\big/\varepsilon\right)\left(\sqrt{\Omega_{ij}\Omega_{ij}}k\big/\varepsilon\right)} \tag{17}$$

$$A = \sqrt{6}\cos\left[\frac{1}{3}\arccos\left(\sqrt{6}W\right)\right], \qquad W = \frac{S_{ij}S_{jk}S_{ki}}{[S_{ij}S_{ij}]^{\frac{3}{2}}}$$

$$U = \sqrt{S_{ij}S_{ij} + \Omega_{ij}\Omega_{ij}} \tag{18}$$

Volume Fraction–Velocity Term

The volume fraction–velocity correlation appearing in Eq. (2) can be modeled similarly to that of the Reynolds stress terms

$$-\overline{F'u_i'} = C_F\upsilon_\tau\frac{\partial\bar{F}}{\partial x_i} \tag{19}$$

where C_F is the correlation coefficient between the fluctuation of volume fraction and velocity components and should be determined. C_F is inversely proportional to the turbulent Schmidt number. However, the simple gradient transport is only appropriate for homogeneous flows where the size of the energy-containing eddies is smaller than the distance over which the gradient varies appreciably. For flows near the interface, where the turbulence is inhomogeneous, a more appropriate model introduced by Lumley[14] that consists of a gradient transport and a convective transport term, which vanishes in homogeneous flows, is used. This model is presented for a passive scalar admixture in inhomogeneous turbulent flows. The model when applied to volume fraction F is

$$-\overline{F'u_i'} = C_F\left[\upsilon_\tau\frac{\partial\bar{F}}{\partial x_i} + \frac{1}{2}\bar{F}\frac{\partial\upsilon_\tau}{\partial x_i}\right] \tag{20}$$

The resulting differential equation for F, after including the turbulence model, may be obtained by inserting Eq. (20) into Eq. (2). The result is

$$\frac{\partial\bar{F}}{\partial t} + \frac{\partial\bar{F}\bar{u}_i}{\partial x_i} = C_F\frac{\partial}{\partial x_i}\left[\nu_\tau\frac{\partial\bar{F}}{\partial x_i} + \frac{1}{2}\bar{F}\frac{\partial\nu_\tau}{\partial x_i}\right] \tag{21}$$

Pressure Term

Modeling of the pressure term, the third term on the right-hand side of Eq. (9), is more complicated. As stated earlier, the pressure fluctuations near the interface may have a significant impact on the shape and topology of the interface. Because the frequency of the turbulent fluctuations is high, the local curvature of the flow is very large, and it may produce large local surface forces at the interface. From the physical point of view, one expects the pressure and the interface location fluctuations, p' and H', to be well correlated.

The approach is based on modeling the instantaneous curvature of the fluctuating interface. The pressure term at the interface, where the surface tension is present, is considered, and the correlation between the fluctuations of the curvature and the interface level is modeled. The average of Eq. (8) can be written as

$$\bar{p} = \overline{(p_1 - p_2)H} + \overline{p_2} = \sigma\overline{\kappa H} + \overline{p_2} \tag{22}$$

where κ is the interface curvature. The first term on the right-hand side can be decomposed into mean and fluctuating parts,

$$\bar{p} = \sigma\bar{\kappa}\bar{H} + \sigma\overline{\kappa'H'} + \overline{p_2} \tag{23}$$

The objective is to model the mean value of the correlation of the fluctuations of curvature and the interface location $\overline{\kappa'H'}$. The fluctuation of H in a control volume is equal to l'/L, where the length l' is the instantaneous fluctuation of the interface level denoted by turbulent integral length scale ℓ (Fig. 1) and L is a physical length, for example, the domain size. In the $\overline{\kappa'H'}$ correlation, we use Taylor microscale Λ as the characteristic length scale for the curvature fluctuations. Thus,

$$\overline{\kappa'H'} = C'(\ell/L\Lambda) \tag{24}$$

where L is a physical length scale, and, in the numerical method, it may be considered the mesh size as just stated. C' is a positive correlation coefficient between H' and κ' and is assumed to be constant. Using the analysis for the homogeneous isotropic turbulence and equating the rate of decay of turbulent kinetic energy to the dissipation rate, following Taylor, we obtain a relation for the Taylor microscale (see Ref. 15)

$$\Lambda = (10\nu k/\varepsilon)^{\frac{1}{2}} \tag{25}$$

Using dimensional analysis, ℓ can be written in terms of k and ε (Ref. 15):

$$\ell = C_\mu(k^{\frac{3}{2}}/\varepsilon) \tag{26}$$

Therefore, Eq. (25) becomes

$$\Lambda/\ell = (10/Re_\tau)^{\frac{1}{2}} \tag{27}$$

where Re_τ is the turbulent Reynolds number defined as

$$Re_\tau = \sqrt{k}\ell\big/\nu = C_\mu(k^2/\nu\varepsilon) = \nu_\tau/\nu \tag{28}$$

As shown in Eq. (28), turbulent Reynolds number Re_τ can be related to the kinematic eddy viscosity ν_τ. Inserting Eq. (27) into Eq. (24) results in

$$\overline{\kappa'H'} = C_p\left(Re_\tau^{\frac{1}{2}}\big/L\right) = (C_p/L)(\nu_\tau/\nu)^{\frac{1}{2}} \tag{29}$$

where C_p is the model constant to be determined. Therefore, comparing Eqs. (9), (10), (23), and (29), one can write

$$\overline{(p_1' - p_2')H'} = \sigma\overline{\kappa'H'} = (C_p\sigma/L)(\nu_\tau/\nu)^{\frac{1}{2}} \tag{30}$$

To further investigate the consistency of this model, some additional points are discussed here. In Eq. (30), L is a physical length scale, for example, the domain size or grid size Δx. On the other hand, because the mean curvature has the maximum value of $(2/\Delta x)$, $1/L$ can be scaled by mean curvature, that is, we can assume that $(1/L \sim \bar{\kappa})$. Thus

$$\overline{(p_1' - p_2')H'} = \sigma\overline{\kappa'H'} = C_p'\sigma\bar{\kappa}(\nu_\tau/\nu)^{\frac{1}{2}} \tag{31}$$

In other words

$$\overline{\kappa'H'} = c'\bar{\kappa}(\nu_\tau/\nu)^{\frac{1}{2}} \tag{32}$$

This means that the unresolved high-frequency small-scale fluctuations of curvature in turbulent flows can be represented by increasing mean curvature $\bar{\kappa}$ by a factor of $(\nu_\tau/\nu)^{1/2}$ due to turbulence effects with the proper coefficient. In fact, this term is larger (and, therefore, more important) for a RANS formulation than an LES formulation with similar flow conditions. This formulation is consistent with Alajbegovic's theory[9] that the unresolved curvature should be proportional to the mean (resolved) curvature with a coefficient of proportionality that is dependent on the subgrid stresses (for LES formalism) that can be represented by ν_τ here. More clearly,

Eq. (31) shows that the surface tension force in turbulent flows is increased by a factor of $(\nu_\tau/\nu)^{1/2}$. On the other hand, according to some experiments performed with polymer additives to water (for high-velocity water jets discharging into still air) such as Hoyt and Taylor's experiment,[16] the spray droplet formation is inhibited by polymer solutions. An explanation for this is that the addition of polymers (such as polyethylene oxide) increases viscosity and, even if we keep the same amount of turbulence intensity, according to Eq. (31), where ν is in the denominator, this suppresses the interfacial breakup.

Alternative Model for Pressure Term

Here we present an alternative method of deriving a model for the third term in the right-hand side of Eq. (9). Similar to what we have for the mean part of the pressure, for the last term in Eq. (9), one may write

$$\overline{(p_1' - p_2')H'} = \sigma_\tau \bar{\kappa} \bar{H} \tag{33}$$

where σ_τ is a new term that we will refer to as the turbulent surface tension coefficient. Unlike the first model where the surface tension coefficient was not changed, and effects of turbulence were represented by a turbulence-induced curvature term, in this model, we have kept the average curvature similar to the laminar calculation, but added a turbulence-induced surface tension effect to the flow. We must show that this alternative model will result in the same concept. To derive a relation for σ_τ, one should examine all of the variables that may affect it. Because the scales that have sizes larger than the Kolmogorov length scale, for example, Taylor microscale, are responsible for the pressure interface fluctuation level correlations, one expects that σ_τ will be related to the characteristics of the turbulent flow in this scale. After careful inspection, we found that σ_τ should depend on the molecular surface tension σ, turbulent kinetic energy k and its disspation rate ε, and a small but energetic length scale, Taylor microscale Λ. There may be some smaller dependencies on other parameters such as density ratio. At present, we have not considered the effects of density and viscosity ratios in our models, and they are lumped into our correlation coefficients. We can conclude that

$$\sigma_\tau = f(\sigma, k, \varepsilon, \Lambda) \tag{34}$$

where f is a function to be determined. By dimensional analysis, one may obtain

$$\sigma_\tau = C_p' \sigma (k^{\frac{3}{2}}/\varepsilon\Lambda) = C_p'' \sigma (Re_\tau)^{\frac{1}{2}} = C_p'' \sigma (\upsilon_\tau/\upsilon)^{\frac{1}{2}} \tag{35}$$

Therefore, Eq. (33) becomes

$$\overline{(p_1' - p_2')H'} = \sigma_\tau \bar{\kappa} \bar{H} = C_p'' \sigma \bar{\kappa} (\upsilon_\tau/\upsilon)^{\frac{1}{2}} \bar{H} \tag{36}$$

When Eqs. (31) and (36) are compared, it is observed that they are basically similar except for the $\bar{H}$ term. It is shown that the surface tension term increases in turbulent flows, and the amount of magnification is proportional to $(\nu_\tau/\nu)^{1/2}$. This magnification is either represented by the fluctuations in curvature with a molecular surface tension coefficient or by a turbulent surface tension coefficient with an average curvature. In both cases, the expressions are nearly identical. For this study, we have used the small-scale curvature formulation of Eq. (30).

Thus far, a model for the volume fraction–velocity correlation (with model constant C_F) and a model for the pressure fluctuation at the interface (with model constant C_p) have been derived. These models should be assessed in different problems for determining the unknown constant coefficients. It is necessary to test them against different experimental data to obtain some globally valid coefficients. Here, a sheared immiscible interface has been simulated for a preliminary examination of the effect of model constants on the interface dynamics.

Numerical Method

A VOF method based on a piecewise linear interface calculation (PLIC), along with a projection method to solve the two-dimensional unsteady incompressible Navier–Stokes equations on a staggered grid and the continuous surface stress method[17] for modeling the interfacial tension, is used in this work. The computational grid is fixed, rectangular, and uniform. The code SURFER is modified and used in this work. The details of the numerical method based on VOF-PLIC and Chorin's projection method for a semi-implicit Navier–Stokes solver, which have been used in this code, are given by Lafaurie et al.[17] The procedure to formulate H and to calculate it numerically is thoroughly given by Shirani et al.[12] The calculation of the volume fraction is somewhat different from the conventional VOF method due to the existence of an extra term in the F equation (2). Equation (21) contains convection and diffusion terms. To solve this equation, it is split into two parts. The convection term is treated by the VOF method, and the diffusion term is solved by means of a finite difference method.

Results and Discussion

To examine the behavior of the models introduced in this paper, two cases are examined here.

Kelvin–Helmholtz Instability

We first consider a sheared immiscible interface between two fluids of equal densities and viscosities. The initial configuration is shown in Fig. 2. The domain size is 2λ in both the horizontal and vertical directions. Boundary conditions are periodic in the horizontal direction and free slip at the top and the bottom. The fluid below the interface is moving to the right with velocity $\Delta U/2$, and the fluid on the top of the interface moves to the left with velocity $\Delta U/2$. The initial perturbation amplitude is equal to 10% of the wavelength of the initial perturbation. The Reynolds and Weber numbers are defined based on the wavelength as $Re = \rho \Delta U \lambda/\mu$ and $We = \rho(\Delta U)^2/(\sigma K) = \rho(\Delta U)^2 \lambda/(2\pi\sigma)$, where K is the wave number. The values of Reynolds number and Weber number are 5×10^5 and 150, respectively. A 128×128 computational grid is used.

Table 1 shows different cases considered here using the standard k–ε (denoted by S) and algebraic (denoted by A) turbulence models and different values for the two coefficients of our free-surface turbulence correlations C_F and C_P. In the first case (case 1 or base case), no turbulence model is used, and both of these coefficients are set to zero ($C_F = C_P = 0$). All of the other cases are compared to this base case. Figure 3a shows the surface evolution for the base case. Columns 1–4 correspond to nondimensional times 1, 2, 2.5, and 3 scaled by $\lambda/\Delta U$.

In cases 2 and 3, the standard k–ε and algebraic turbulence models are used, respectively, without correlation models ($C_F = C_P = 0$),

Table 1 Models used and model coefficient values for different cases

	Case														
Characteristic	1 (base)	2	3	4	5	6	7	8	9	10	11	12	13	14	15
Turbulence model	——	S	A	S	S	S	A	A	A	S	S	A	A	S	A
C_F	0	0	0	0	0	0	0	0	0	1	5	1	5	5	5
C_P	0	0	0	0.5	1	2	0.5	1	2	0	0	0	0	2	2

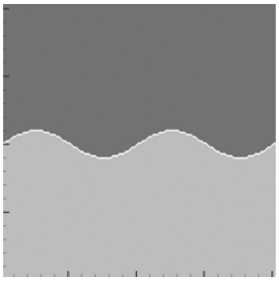

Fig. 2 Initial flowfield.

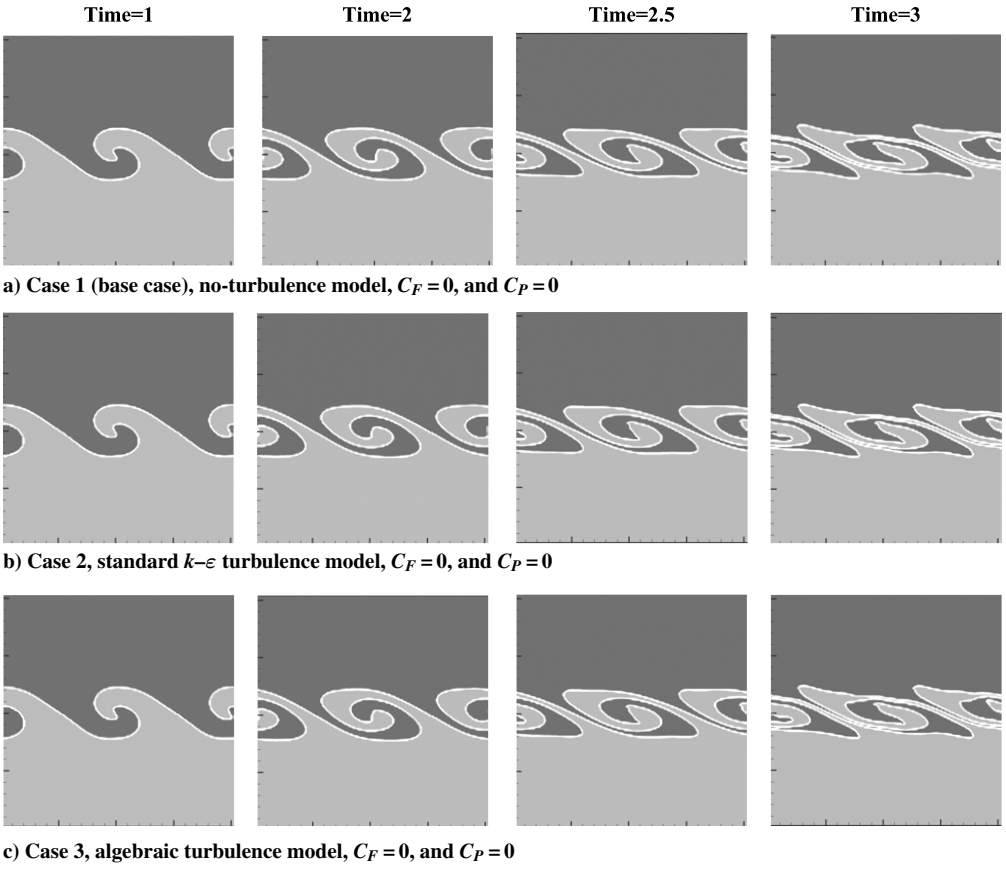

Fig. 3 Effect of employing only turbulence models without correlations ($C_F = 0$ and $C_P = 0$) on surface evolution; nondimensional times 1, 2, 2.5, and 3 scaled by $\lambda/\Delta U$.

and results are shown in Figs. 3b and 3c. When a turbulence model is implemented without using any correlation for the effect of turbulence on the interface, no significant effect (at least qualitatively visible) is observed.

Cases 4–6 show the effect of the pressure model coefficient on the flow characteristics. Results are shown in Fig. 4. In these cases, a standard k–ε turbulence model is used and C_P changes from 0.5 to 2 whereas C_F is kept at 0 for all cases (Figs. 4a–4c). When the flow patterns at time = 2.5 are compared, it can be seen that increasing C_P (increasing the effect of the pressure term) accelerates the rate of thinning of ligaments formed. In Fig. 4c, one can see that, for a large coefficient of $C_P = 2$, ligaments break very quickly. Because we have not conducted a detailed grid dependency test of the breakup, we cannot predict the exact breaking condition, but it is clear that an increase in C_P results in faster breakup. The ligaments that are separated undergo further breakup and form smaller drops. More rapid breakup results in the droplet dispersion. Therefore, the mixing layer becomes thicker.

Figure 5 (cases 7–9) is similar to Fig. 4, except that the algebraic turbulence model is used. Again, the effect of increasing C_P on the thinning of ligaments can be observed. In Fig. 5, however, the rate of ligament thinning is lower than that in Fig. 4. This can be because the algebraic turbulence model gives a smaller kinematic eddy viscosity ν_τ than the standard k–ε turbulence model. Therefore, from Eq. (30), it is obvious that the pressure term is smaller for an algebraic model having the same C_P. Also, comparing Figs. 4a and 5b, one can see that they are quite similar. This means that the pressure term effect for the standard k–ε model with $C_P = 0.5$ is nearly equal to that of algebraic model with $C_P = 1$. Therefore, an increase in C_P in effect increases the mixing similar to the effect of ν_τ. Given Eq. (30), the left-hand side of the equation can be modified by either changing C_P or ν_τ.

Cases 10–13, Figs. 6 and 7, show the effect of the volume fraction–velocity correlation, where C_F changes from 1 to 5, whereas C_P is kept at 0. It can be seen that, at a small value of $C_F = 1$, interface shape is not much affected (or at least its effect cannot be observed qualitatively) by this model. Increasing C_F to 5 increases the rate of diffusion of fluids into each other. Because the volume fraction–velocity correlation depends on the ν_τ, as shown in Eq. (20), again the effect of C_F is greater in the standard k–ε model than in the algebraic model. In contrast to the pressure model that accelerates the rate of thinning of the ligaments, the volume fraction–velocity model increases the thickness of the ligaments formed.

Cases 14 and 15 (Fig. 8) show the combined effect of both correlations using $C_F = 5$ and $C_P = 2$. In Fig. 8a the standard k–ε model is used, whereas in Fig. 8b, the algebraic model is used. Here, the volume fraction–velocity model tends to thicken the ligaments and prevents them from breaking. In contrast, the pressure model tends to detach the ligaments and form smaller ligaments. In these cases, the effect of the pressure model is dominant. Comparing case 14 with case 6 ($C_F = 0$ and $C_P = 2$), one can see that, in case 14, the ligaments are thicker, and they are less likely to disperse compared to case 6.

Plane Turbulent Liquid Jet

To validate the models introduced in this paper, a simulation of a plane turbulent water jet injected into still air is performed and compared to the experimental results by Sallam et al.[10] The mean jet exit velocity and the jet diameter in the simulation are taken from the experiments. This study can give an overall picture of the flow and some spray quantities such as the amount of jet diffusion. Because of symmetry of the flow conditions, only one-half of the domain is considered. A 128×64 grid (domain size $12b \times 6b$, where b is the nozzle half-width) is employed. Given a hydraulic diameter (approximated as $4b$) of $d_h = 13.5$ mm, and a mean jet exit average velocity ($\bar{u}_0$) of 15.8 m/s, the Reynolds and Weber numbers based on liquid properties are 2.38×10^5 and 47,500, respectively. The boundaries are inflow at the top, no gradient outlet at the bottom, symmetry at the right (because we are solving for one-half of the

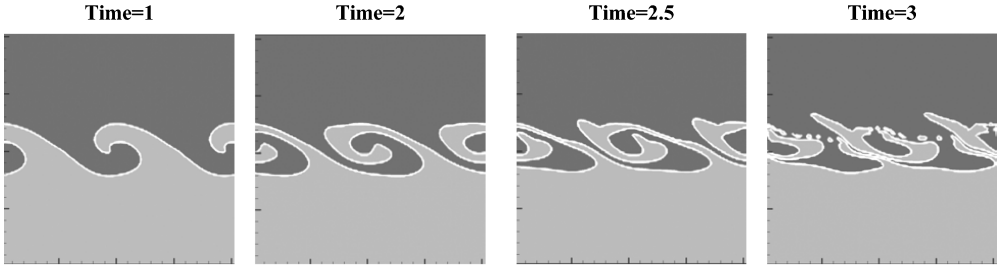

a) Case 4, standard k–ε turbulence model, $C_F = 0$, and $C_P = 0.5$

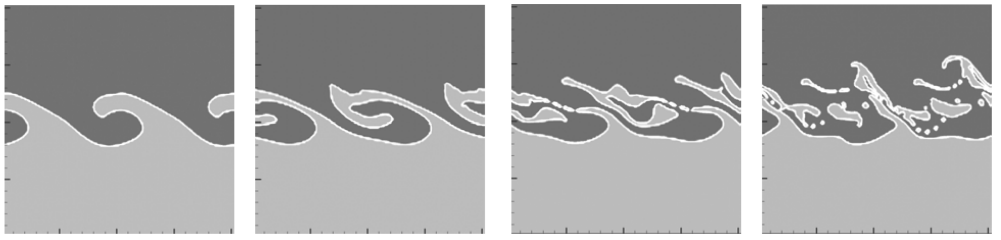

b) Case 5, standard k–ε turbulence model, $C_F = 0$, and $C_P = 1$

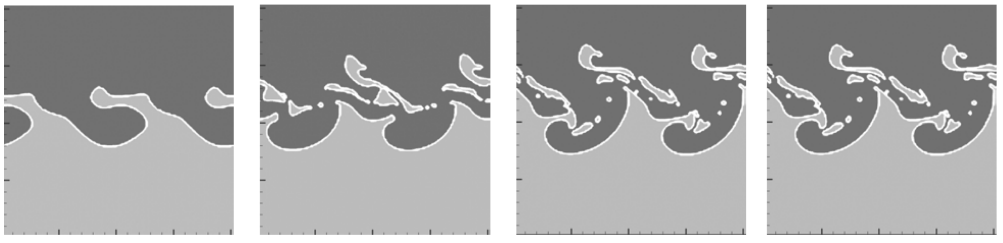

c) Case 6, standard k–ε turbulence model, $C_F = 0$, and $C_P = 2$

Fig. 4 Effect of pressure model coefficient C_P on surface evolution for standard k–ε model; nondimensional times 1, 2, 2.5, and 3 scaled by $\lambda/\Delta U$.

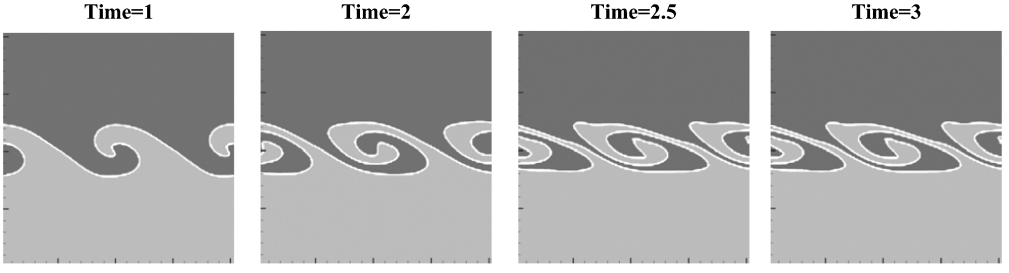

a) Case 7, algebraic turbulence model, $C_F = 0$, and $C_P = 0.5$

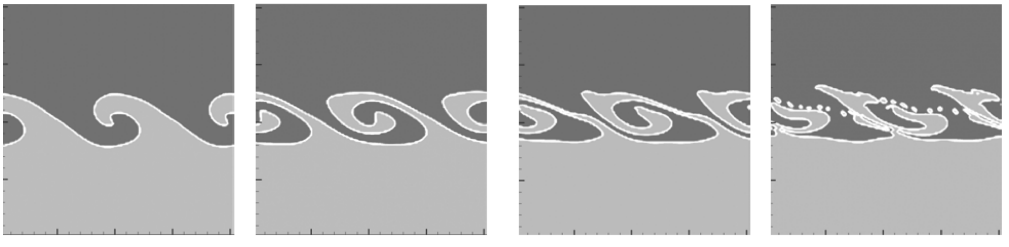

b) Case 8, algebraic turbulence model, $C_F = 0$, and $C_P = 1$

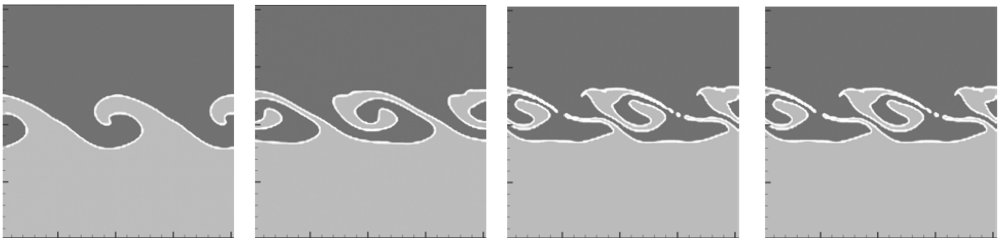

c) Case 9, algebraic turbulence model, $C_F = 0$, and $C_P = 2$

Fig. 5 Effect of pressure model coefficient C_P on surface evolution for algebraic model; nondimensional times 1, 2, 2.5, and 3 scaled by $\lambda/\Delta U$.

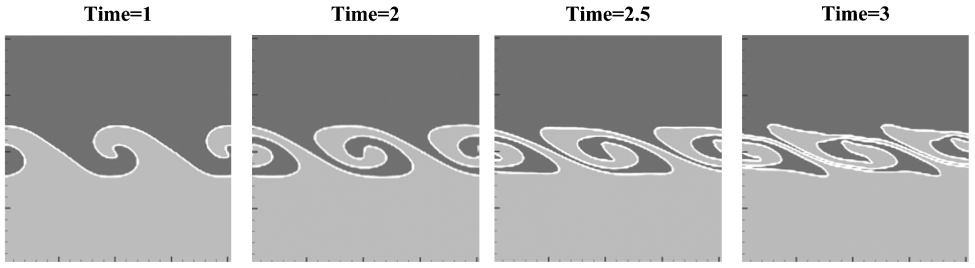

a) Case 10, standard k–ε turbulence model, $C_F = 1$, and $C_P = 0$

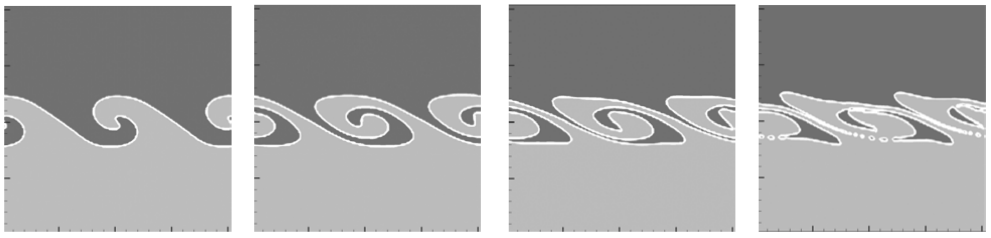

b) Case 11, standard k–ε turbulence model, $C_F = 5$, and $C_P = 0$

Fig. 6 Effect of volume fraction–velocity model coefficient C_F on surface evolution for standard k–ε model; nondimensional times 1, 2, 2.5, and 3 scaled by $\lambda/\Delta U$.

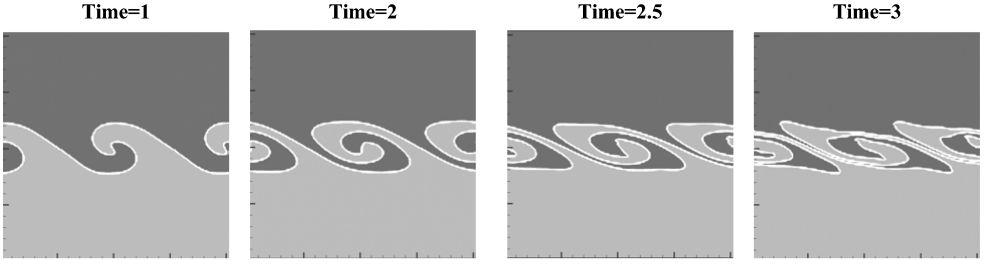

a) Case 12, algebraic turbulence model, $C_F = 1$, and $C_P = 0$

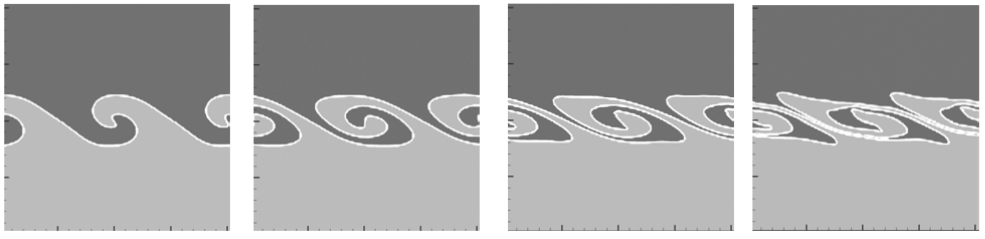

b) Case 13, algebraic turbulence model, $C_F = 5$, and $C_P = 0$

Fig. 7 Effect of volume fraction–velocity model coefficient C_F on surface evolution for algebraic model; nondimensional times 1, 2, 2.5, and 3 scaled by $\lambda/\Delta U$.

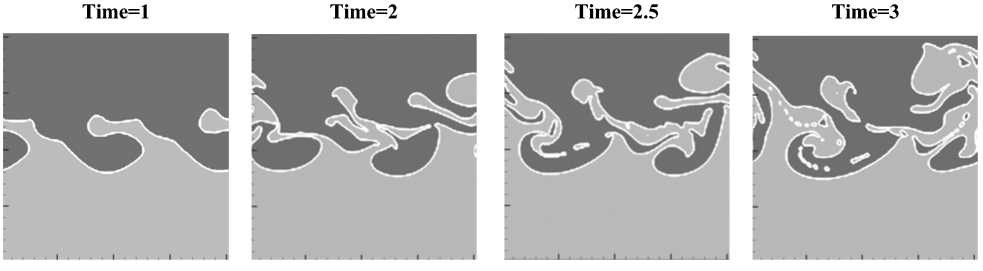

a) Case 14, standard k–ε turbulence model, $C_F = 5$, and $C_P = 2$

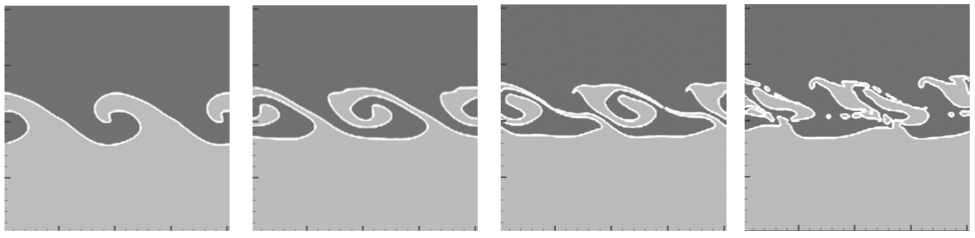

b) Case 15, algebraic turbulence model, $C_F = 5$, and $C_P = 2$

Fig. 8 Effect of employing both models on surface evolution; nondimensional times 1, 2, 2.5, and 3 scaled by $\lambda/\Delta U$.

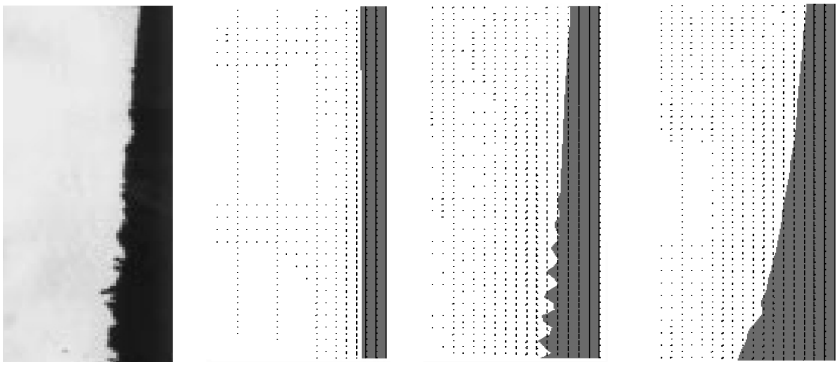

a) b) c) d)

Fig. 9 Results of a) experiment[17] and numerical simulation for b) $C_F = 0$ and $C_P = 0$, c) $C_F = 0.1$ and $C_P = 1$, and d) $C_F = 0.2$ and $C_P = 1$; vectors are scaled by $\bar{u}_0$.

domain) and free at the left boundary. The algebraic turbulence model is used with the boundary conditions similar to those by Shih et al.,[13] and the inlet turbulence intensity is assumed to be 1%.

The main issue is to find a set of coefficients that can provide good results for a wide range of experimental conditions. Figure 9 shows three cases with different model constants, as well as the experimental result. The simulations show the surface of liquid jet along with the velocity vectors. Figure 9a shows the shadowgraphs of the experiments conducted by Sallam et al.[10] The wave formation and interface structure can be observed. Figure 9b shows a case in which the turbulence models developed here are eliminated by setting the model coefficients to zero, that is, $C_F = 0$ and $C_P = 0$. The results show that the jet does not spread. However, when the turbulence models are included, the jet spreads significantly. Figure 9c shows the results for the case where the turbulence equations are used and the coefficient values are $C_F = 0.1$ and $C_P = 1$. As is seen, this set of coefficients provides a satisfactory result that is comparable to that of the experiment. Increasing C_F to 0.2 causes more diffusion and spreading of the jet (Fig. 9d), as is also observed in the Kelvin–Helmholtz instability case. From the results obtained in this case, we can conclude that the models introduced in this paper with coefficients $C_F = 0.1$ and $C_P = 1$ produce reasonable results, and the spreading rate of the turbulent jet is correctly predicted.

Conclusions

The governing equations for description of the turbulent interfacial flows, based on the Reynolds-averaged equations of motion for two fluids with interfaces, is developed. The present study indicates that it is difficult to capture the real interface spreading in turbulent liquid jets using the presently available turbulence models. For this purpose, two different models are developed to include the turbulence interface effects in standard turbulence models. These are

$$\overline{(p_1' - p_2')H'} = \sigma\overline{\kappa' H'} = (C_p \sigma / L)(\nu_\tau / \nu)^{\frac{1}{2}}$$

which includes the effects of the pressure interface fluctuation model and

$$-\overline{F' u_i'} = C_F \left[\upsilon_\tau \frac{\partial \bar{F}}{\partial x_i} + \frac{1}{2} \bar{F} \frac{\partial \upsilon_\tau}{\partial x_i} \right]$$

which is the correlation for volume fraction–velocity fluctuations. In this paper, we have investigated the effects of the coefficients C_F and C_P on the interface shape evolution and the spreading rate of a turbulent liquid jet using standard k–ε and algebraic turbulence models. The findings are as follows:

1) The ratio of small-scale curvature to the resolved curvature is proportional to $(\nu_\tau / \nu)^{1/2}$, which is a property of the turbulent flow. This small-scale curvature can be used with the molecular surface tension coefficient.

2) In an alternative method of modeling unresolved surface tension forces, a new property referred to as the turbulent surface tension coefficient σ_τ is introduced. This quantity is proportional to the molecular surface tension with the proportionality being a function of $(\nu_\tau / \nu)^{1/2}$. The turbulent surface tension coefficient is used with the averaged curvature to model the unresolved effects of interfacial tension forces.

3) The unresolved interface motion is also taken into account, and it is found that the model makes the interface more diffusive.

The models developed here are used in investigating a sheared interface between two immiscible fluids, as well as simulating a plane turbulent water jet. The results show that, for the sheared interface case, the turbulence in the flow can generate significant interface fluctuations. These fluctuations grow and result in the breakup of ligaments from the interface. It is shown that the flow pattern is quite sensitive to the values of the model coefficients. A set of preliminary coefficients, $C_F = 0.1$ and $C_P = 1$, were found that correctly predict the spreading rate of the plane turbulent jet tested here.

Note that the numerical simulations conducted in this paper are mainly done for the demonstration of the importance of the model constants in turbulent interfacial flow simulations. Further tests are required to determine the global model coefficients and to derive more comprehensive models.

Acknowledgments

This project was supported by Natural Sciences and Engineering Research Council of Canada, Materials and Manufacturing Ontario, and Alstom Canada.

References

[1]Hong, W. L., and Walker, D. T., "Reynolds-Averaged Equations for Free-Surface Flows with Application to High-Froude-Number Jet Spreading," *Journal of Fluid Mechanics*, Vol. 417, 2000, pp. 183–209.

[2]Banerjee, S., "Modeling Considerations for Turbulent Multiphase Flows," *Engineering Turbulence Modeling and Experiments*, edited by W. Rodi and E. N. Ganic, Elsevier Science, New York, 1990, pp. 831–866.

[3]Lopez de Bertodano, M., Jones, O. C., and Lahey, R. T., "Development of k–ε Model for Bubbly Two-Phase Flow," *Journal of Fluids Engineering*, Vol. 116, No. 1, 1994, pp. 128–134.

[4]Lahey, R. T., and Drew, D. A., "An Analysis of Two-Phase Flow and Heat Transfer Using a Multidimensional, Multi-Field Computational Fluid Dynamics (CFD) Model," Japan/U.S. Seminar on Two-Phase Flow Dynamics, June 2000.

[5]Walker, D. T., and Chen, C. Y., "Evaluation of Algebraic Stress Modeling in Free-Surface Jet Flows," *Free-Surface Turbulence*, edited by E. P. Rood and J. Katz, FED-Vol. 181, American Society of Mechanical Engineers, New York, 1994, pp. 83–95.

[6]Lin, P., and Liu, P. L. F., "A Numerical Study of Breaking Waves in the Surf Zone," *Journal of Fluid Mechanics*, Vol. 359, 1998, pp. 239–264.

[7]Klein, M., and Janicka, J., "Large-Eddy Simulation of the Primary Breakup of a Spatially Developing Liquid Film," 9th International Conf. on Liquid Atomization and Spray Systems, Paper 0204, July 2003.

[8]Herrmann, M., "Modeling Primary Breakup: A Three-Dimensional Eulerial Level Set/Vortex Sheet Method for Two-Phase Interface Dynamics," *Annual Research Briefs*, Center for Turbulence Research, Stanford Univ., Stanford, CA, 2003, pp. 185–196.

[9]Alajbegovic, A., "Large Eddy Simulation Formalism Applied to Multiphase Flows," American Society of Mechanical Engineers, Paper FEDSM 2001-18192, New York, May–June 2001.

[10]Sallam, K. A., Dai, Z., and Faeth, G. M., "Drop Formation at the Surface of Plane Turbulent Liquid Jets in Still Gases," *International Journal of Multiphase Flow*, Vol. 25, Nos. 6–7, 1999, pp. 1161–1180.

[11]Hirt, C. W., and Nichols, B. D., "Volume of Fluid (VOF) Method for the Dynamics of Free Boundaries," *Journal of Computational Physics*, Vol. 39, No. 1, 1981, pp. 201–225.

[12]Shirani, E., Ashgriz, N., and Mostaghimi, J., "Interface Pressure Calculation Based on Conservation of Momentum for Front Capturing Methods," *Journal of Computational Physics*, Vol. 203, No. 1, 2005, pp. 154–175.

[13]Shih, T.-H., Zhu, J., and Lumley, J. L., "A New Reynolds Stress Algebraic Equation Model," *Computer Methods in Applied Mechanics and Engineering*, Vol. 125, No. 1, 1995, pp. 287–302.

[14]Lumley, J. L., "Modeling Turbulent Flux of Passive Scalar Quantities in Inhomogeneous Flows," *Physics of Fluids*, Vol. 18, No. 6, 1975, pp. 619–621.

[15]Wilcox, D. C., *Turbulence Modeling for CFD*, DCW Industries, La Canada, CA, 2000, pp. 44, 45.

[16]Hoyt, J. W., and Taylor, J. J. "Turbulence Structure in a Water Jet Discharging in Air," *Physics of Fluids*, Vol. 20, No. 10, 1977, pp. S253–S257.

[17]Lafaurie, B., Nardone, C., Scardovelli, R., Zaleski, S., and Zanetti, G., "Modeling Merging and Fragmentation in Multiphase Flows with SURFER," *Journal of Computational Physics*, Vol. 113, No. 1, 1994, pp. 134–147.

S. Aggarwal
Associate Editor